Magnetic Feedstock for Fused Deposition Modeling

Subjects: Engineering, Mechanical

Contributor: Guido Ehrmann , Tomasz Blachowicz , Andrea Ehrmann

Three-dimensional printing enables building objects shaped with a large degree of freedom. Additional functionalities can be included by modifying the printing material, e.g., by embedding nanoparticles in the molten polymer feedstock, the resin, or the solution used for printing, respectively. Such composite materials may be stronger or more flexible, conductive, magnetic, etc.

3D-printed FDM magnetic composites

1. Three-Dimensional Printing Techniques

Generally, the feedstock for 3D printing can take the form of a filament/wire (e.g., FDM printing), a powder (e.g., selective laser sintering, SLS), or a fluid (e.g., SLA, PolyJet Matrix [1]), in addition to two- or more-component methods in which a binder and a powder or other components are combined (e.g., binder jetting [2]). Depending on the exact way of processing the feedstock, several technologies can be defined.

FDM is most common in inexpensive printers used at home or in school or university. A polymer filament of defined diameter is pulled into a hot-end, molten, and pressed through a nozzle. The molten polymer is placed along defined paths to form an object layer by layer [3][4]. For metals, a similar process is wire arc additive manufacturing [5].

SLS works by fusing subsequent layers in a powder bed and can not only be used to process polymers, but also metals or ceramics [6][7]. Other powder-bed-based techniques are, e.g., selective laser melting, direct metal laser sintering, and electron beam melting [8].

Among the photopolymerization techniques, SLA is the oldest and probably the most common one. In this technique, the printing bed is lowered into a basin filled with resin, and the highest layer is polymerized by laser light, before the printing bed is lifted by one layer height, and the next layer is polymerized [9]. Digital light processing (DLP) uses a digital micro-mirror device in the light path, enabling light exposure of a full layer at the same time [10]. In the PJM technology, objects are created on top of a printing bed, where a liquid polymer resin is sprayed on desired positions and cured by UV light [1]. Even more exact shapes can be reached by two-photon or multi-photon polymerization, where a strongly focused laser enables absorbing two or more photons simultaneously, in this way strictly limiting the area where polymerization can take place [11][12].

2. Magnetic Composites for Fused Deposition Modeling

Generally, many magnetic materials can be embedded in a polymeric feedstock for FDM printing, from nanoparticles to microflakes or fibers in different dimensions, and from soft to hard magnetic materials. Similarly, diverse polymers can be applied, most of them typical for FDM printing. Common soft magnetic materials used, e.g., in electric machines to guide magnetic fields, are Si-Fe alloys (also printable without a polymer matrix [13]), Ni-Fe alloys (e.g., permalloy [14]), nickel [15], magnetite [16][17], NiZn ferrites [18][19], MnZn ferrites [20], etc. Hard magnetic materials, characterized by large coercivity and ideally also large remanence, are used for technical permanent magnets and often include rare-earth elements, such as neodymium-iron-boron (NdFeB)-based magnets [21] or magnetic ceramics such as barium hexaferrite [22] or strontium hexaferrite, while manganese-based alloys such as MnBi, MnAl, or MnGa, alnico magnets, and iron nitride ($Fe_{16}N_2$) are less often used in 3D-printed polymer/magnetic composites.

Due to the interest in 3D printing freeform magnets with different magnetic properties, several research groups developed a magnetic feedstock for FDM printing, often based on polymer/ferrite composites [23]. Palmero et al. described the preparation of a polyethylene (PE)/MnAlC composite filament [24]. For this, they prepared a magnetic MnAlC powder by gas-atomization, resulting in spherical particles of diameters below 36 µm, which were embedded in a PE matrix by dispersing/dissolving both materials in toluene, so that a polymeric matrix was formed around the MnAlC particles. The resulting pellets were extruded into a magnetic filament with a diameter of 1.75 mm, suitable for standard FDM printing, and showed coercive fields around 1.5 kOe [24]. The filament and its inner structure are depicted in **Figure 1**. The research group showed in a subsequent paper a filling factor of even 80 wt%, which they attributed to an optimum ratio of fine to coarse particles, enabling the production of freeform permanent magnets without rare earth materials [25].

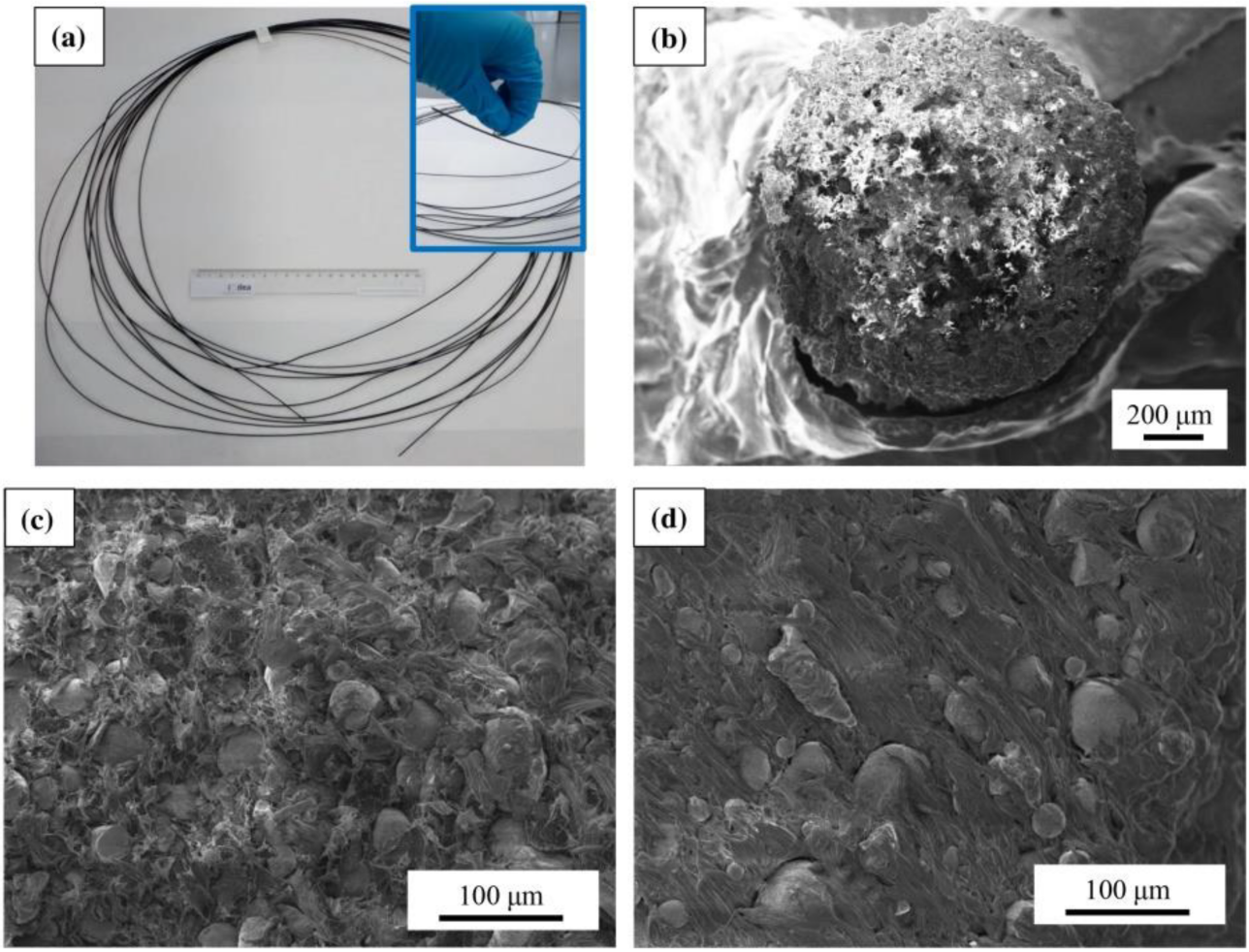

Figure 1. (**a**) Extruded MnAlC–PE magnetic filament (with a 20 cm ruler for scale comparison); SEM images of (**b**) the circular cross-section of the MnAlC-PE filament, and internal filament morphology for filling factors (**c**) 72.3% and (**d**) 52.1%. From [24], originally published under a CC-BY license.

The production of a magnetic FDM feedstock containing polyethylene was also reported by Arbaoui et al. who used permalloy, or more exactly, $Ni_{81}Fe_{19}$, as magnetic particles [26]. These commercially available spherical particles had diameters of a few microns, i.e., smaller than those used by Palmero et al. [24][25]. Composite materials were prepared by propeller mixing in a molten state as well as by using a twin screw extruder, with filler volume fractions between 10% and 40%. From the composite with 30 vol% permalloy, an FDM filament with a diameter of 3 mm was prepared and used to print a small parallelepiped, which was not further investigated [26].

Another polymer often used to prepare magnetic FDM feedstock is acryl butadiene styrene (ABS). Hanemann et al., e.g., prepared a composite feedstock from ABS and barium ferrite ($BaFe_{12}O_{19}$), which is a ferrimagnetic material [27]. The commercially available barium ferrite had an average particle size of 500 nm, i.e., much smaller than the previously discussed MnAlC or permalloy microparticles. The composite material was produced in a mixer-kneader unit by adding a surfactant to improve the surface coverage of the nanoparticles, before a filament extruder was used to prepare the final FDM filament with a diameter of 1.75 mm. Among these filaments (**Figure 2**), those with up to 30 vol% barium ferrite could be used to print samples with sufficient quality on a commercial

FDM printer. Coercivities were found in the range of 11 kA/m for 10 vol% barium ferrite up to 29 kA/m for 35 vol% barium ferrite.

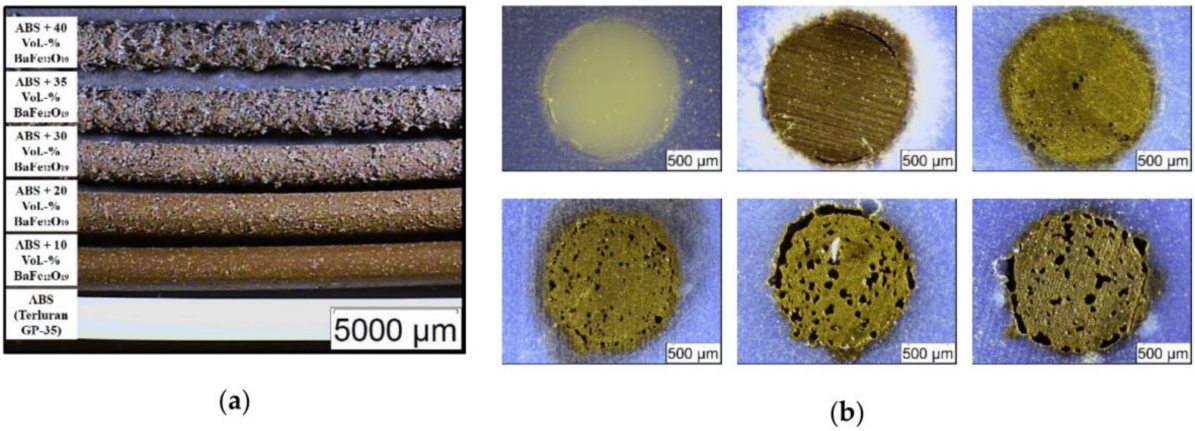

Figure 2. Microscopic images of (**a**) extruded filaments with different solid loadings; (**b**) polished cross-sections with increasing filler content. Upper row: Pure acryl butadiene styrene (ABS), 10 vol.% and 20 vol.% ferrite; lower row: 30 vol.%, 35 vol.%, and 40 vol.% ferrite. From [27], originally published under a CC-BY license.

Gas-atomized stainless-steel alloy particles of diameters around 25 µm were also mixed with ABS to prepare a composite feedstock [28]. For this, ABS pellets were dissolved in acetone, before the metallic particles were added under stirring, and stirring was continued until the acetone was fully evaporated. The resulting composites had stainless-steel volume ratios of 50–90% and were further extruded to filaments with a diameter of 1.75 mm. The filaments showed small coercive fields around 52–55 Oe, with the values of the printed objects being very similar to those of the original stainless-steel powder. While FDM printing from these filaments was successful, the authors nevertheless mentioned future approaches to improve the resolution of the 3D-printed objects.

A similar study with stainless-steel micropowder with an average diameter of 6 µm, compounded in ABS, was performed by heated kneading of ABS and the steel micropowder, followed by extrusion of FDM filaments with a diameter of 1.75 mm [29]. The authors report printing with these filaments for magnetic fillers up to 40 vol%. Coercivities were found around 1.5–4.3 kA/m in this investigation.

Other combinations of polymers and magnetic nano- or microparticles are also reported in the literature. Amongst them, poly(lactic acid) (PLA) was blended with magnetite (Fe_3O_4) and partly with additional poly(vinyl chloride) (PVC) and wood powder [30][31][32]. From the feedstock prepared by twin screw extrusion, filaments with 20 wt% magnetite were prepared and investigated in terms of mechanical and magnetic properties. They showed coercive fields around 84 Oe for PLA as the matrix and of approx. 75 Oe for the hybrid matrix.

While the aforementioned coercive fields are relatively small, much larger values can be found for rare-earth magnetic alloys, such as NdFeB. Pigliaru et al. mixed the high-temperature polymer poly(ether ether ketone) (PEEK) with NdFeB flakes of average thickness 35 µm and coercive fields of 440–496 kA/m after magnetization [33]. Filaments with a diameter of 1.75 mm were prepared by mixing both components in a planetary mixer, followed

by single-screw extrusion at 340 °C. The filaments contained 25–75 wt% of NdFeB. For FDM printing, a special high-temperature printer from Indmatec was used to reach the necessary nozzle temperature of 100 °C. The authors reported that while 25 wt% of NdFeB was still printable with the common nozzle diameter of 0.4 mm, this had to be changed to a nozzle with a diameter of 0.8 mm for the filament containing 50 wt% NdFeB due to the high viscosity of this melt, and the filament with 75 wt% NdFeB could not be printed successfully. Interestingly, while the printed samples with 25 wt% NdFeB had a similar coercive field as the original powder of 413 kA/m, the sample with 50 wt% NdFeB had a significantly reduced coercive field of approx. 167 kA/m, which the authors attributed to a reduced orientation of the magnetic flakes, in this case, due to the larger nozzle.

As these examples show, different combinations of polymer and magnetic nano-/microparticles were shown to be suitable as a feedstock for magnetic FDM filaments. However, while FDM printing has a broad area of applications, the finer structures available by photopolymerization may be more suitable for well-defined magnetic object shapes. The next section, thus, introduces possibilities to prepare magnetic photopolymers, but also other feedstock for different 3D printing techniques.

References

1. Kozior, T.; Kundera, C. Viscoelastic Properties of Cell Structures Manufactured Using a Photo-Curable Additive Technology—PJM. Polymers 2021, 13, 1895.
2. Mostafaei, A.; Elliott, A.M.; Barnes, J.E.; Li, F.Z.; Tan, W.; Cramer, C.L.; Nandwana, P.; Chmielus, M. Binder jet 3D printing—Process parameters, materials, properties, modeling, and challenges. Prog. Mater. Sci. 2021, 119, 100707.
3. Noorani, R. Rapid Prototyping: Principles and Applications; John Wiley & Sons: Hoboken, NJ, USA, 2005.
4. Durgun, I.; Ertan, R. Experimental investigation of FDM process for improvement of mechanical properties and production cost. Rapid Prototyp. J. 2014, 20, 228–235.
5. Bartsch, H.; Kühne, R.; Citarelli, S.; Schaffrath, S.; Feldmann, M. Fatigue analysis of wire arc additive manufactured (3D printed) components with unmilled surface. Structures 2021, 31, 576–589.
6. Tan, K.H.; Chua, C.K.; Leong, K.F.; Cheah, C.M.; Gui, W.S.; Tan, W.S.; Wiria, F.E. Selective laser sintering of biocompaticle polymers for applications in tissue engineering. Bio-Med. Mater. Eng. 2005, 15, 113–124.
7. Zhou, W.Y.; Lee, S.H.; Wang, M.; Cheung, W.L.; Ip, W.Y. Selective laser sintering of porous tissue engineering scaffolds from poly(L-lactide)/carbonated hydroxyapatite nanocomposite microspheres. J. Mater. Sci. Mater. Med. 2008, 19, 2535–2540.

8. Awad, A.; Fina, F.; Goyanes, A.; Gaisford, S.; Basit, A.W. Advances in powder bed fusion 3D printing in drug delivery and healthcare. Adv. Drug Deliv. Rev. 2021, 174, 406–424.
9. Wang, Z.J.; Abdulla, R.; Parker, B.; Samanipour, R.; Ghosh, S.; Kim, K.Y. A simple and high-resolution stereolithography-based 3D bioprinting system using visible light crosslinkable bioinks. Biofabrication 2015, 7, 045009.
10. Kadry, H.; Wadnap, S.; Xu, C.X.; Ahsan, F. Digital light processing (DLP) 3D-printing technology and photoreactive polymers in fabrication of modified-release tablets. Eur. J. Pharm. Sci. 2019, 135, 60–67.
11. Kumi, G.; Yanez, C.; Belfield, K.D.; Fourkas, J.T. High-speed multiphoton absorption polymerization: Fabrication of microfluidic channels with arbitrary cross-sections and high aspect ratios. Lab Chip 2010, 8, 1057–1060.
12. Straub, M.; Gu, M. Near-infrared photonic crystals with higher-order bandgaps generated by two-photon photopolymerization. Opt. Lett. 2002, 27, 1824–1826.
13. Garibaldi, M.; Ashcroft, I.; Simonelli, M.; Hague, R. Metallurgy of high-silicon parts produced using selective laser melting. Acta Mater. 2016, 110, 207–216.
14. Shi, Q.K.; Chen, H.H.; Pang, K.X.; Yao, Y.; Su, G.D.; Liang, F.; Zhou, N.J. Permalloy/polydimethylsiloxane nanocomposite inks for multimaterial direct ink writing of gigahertz electromagnetic structures. J. Mater. Chem. C 2020, 8, 15099–15104.
15. Stottlemire, B.J.; Miller, J.D.; Whitlow, J.; Huayamares, S.G.; Dhar, P.; He, M.; Berkland, C.J. Remote Sensing and Remote Actuation via Silicone–Magnetic Nanorod Composites. Adv. Mater. Technol. 2021, 6, 2001099.
16. Leigh, S.J.; Purssell, C.P.; Billson, D.R.; Hutchins, D.A. Using a magnetite/thermoplastic composite in 3D printing of direct replacements for commercially available flow sensors. Smart Mater. Struct. 2014, 23, 095039.
17. Calascione, T.M.; Fischer, N.A.; Lee, T.J.; Thatcher, H.G.; Nelson Cheeseman, B.B. Controlling magnetic properties of 3D-printed magnetic elastomer structures via fused deposition modeling. AIP Adv. 2021, 11, 025223.
18. Ding, C.; Liu, L.B.; Mei, Y.H.; Ngo, K.D.T.; Lu, G.-Q. Magnetic paste as feedstock for additive manufacturing of power magnetics. In Proceedings of the 2018 IEEE Applied Power Electronics Conference and Exposition (APEC), San Antonio, TX, USA, 4–8 March 2018; IEEE: Piscataway, NJ, USA, 2018; pp. 615–618.
19. Shamray, I.I.; Buz’ko, V.Y.; Goryachko, A.I. Changes in the Structure and Properties of Nickel-Zinc Spinel Nanoferrites Series for 3D-Printing. IOP Conf. Ser. Mater. Sci. Eng. 2020, 969, 012101.

20. Chi, J.C.; Blanco, B.A.; Bruno, G.; Günster, J.; Zocca, A. Self-Organization Postprocess for Additive Manufacturing in Producing Advanced Functional Structure and Material. Adv. Eng. Mater. 2021, 24, 2101262.
21. Li, L.; Tirado, A.; Nlebedim, I.C.; Rios, O.; Post, B.; Kunc, V.; Lowden, R.R.; Lara-Curzio, E.; Fredette, R.; Ormerod, J.; et al. Big Area Additive Manufacturing of High Performance Bonded NdFeB Magnets. Sci. Rep. 2016, 6, 36212.
22. Sukthavorn, K.; Phengphon, N.; Nootsuwan, N.; Jantaratana, P.; Veranitisagul, C.; Laobuthee, A. Effect of silane coupling on the properties of polylactic acid/barium ferrite magnetic composite filament for the 3D printing process. J. Appl. ‘Polym. Sci. 2021, 138, 50965.
23. Wang, Y.Q.; Castles, F.; Grant, P.S. 3D Printing of NiZn ferrite/ABS Magnetic Composites for Electromagnetic Devices. MRS Proc. 2015, 1788, 29–35.
24. Palmero, E.M.; Rial, J.; de Vicente, J.; Camarero, J.; Skarman, B.; Vidarsson, H.; Larsson, P.-O.; Bollero, A. Development of permanent magnet MnAlC/polymer composites and flexible filament for bonding and 3D-printing technologies. Sci. Technol. Adv. Mater. 2018, 19, 465–473.
25. Palmero, E.M.; Casaleiz, D.; de Vicente, J.; Skarman, B.; Vidarsson, H.; Larsson, P.-O.; Bollero, A. Effect of particle size distribution on obtaining novel MnAlC-based permanent magnet composites and flexible filaments for 3D-printing. Addit. Manuf. 2020, 33, 101179.
26. Arbaoui, Y.; Agaciak, P.; Chevalier, A.; Laur, V.; Maalouf, A.; Ville, J.; Roquefort, P.; Aubry, T.; Queffelec, P. 3D printed ferromagnetic composites for microwave applications. J. Mater. Sci. 2017, 52, 4988–4996.
27. Hanemann, T.; Syperek, D.; Nötzel, D. 3D Printing of ABS Barium Ferrite Composites. Materials 2020, 13, 1481.
28. Palmero, E.M.; Casaleiz, D.; de Vicente, J.; Hernández-Vicen, J.; López-Vidal, S.; Ramiro, E.; Bollero, A. Composites based on metallic particles and tuned filling factor for 3D-printing by Fused Deposition Modeling. Compos. Part A Appl. Sci. Manuf. 2019, 124, 105497.
29. Khatri, B.; Lappe, K.; Noetzel, D.; Pursche, K.; Hanemann, T. A 3D-Printable Polymer-Metal Soft-Magnetic Functional Composite—Development and Characterization. Materials 2018, 11, 189.
30. Kumar, S.; Singh, R.; Singh, T.P.; Batish, A. On process capability comparison of hybrid and multi blend PLA matrix composite: Magnetic and surface properties view point. Mater. Today Proc. 2020, 28, 521–525.
31. Kumar, S.; Singh, R.; Singh, T.P.; Batish, A. Investigations of polylactic acid reinforced composite feedstock filaments for multimaterial three-dimensional printing applications. Proc. Inst. Mech. Eng. Part C J. Mech. Eng. Sci. 2019, 233, 5953–5965.

32. Kumar, S.; Singh, R.; Singh, T.P.; Batish, A. Investigations for magnetic properties of PLA-PVC-Fe3O4-wood dust blend for self-assembly applications. J. Thermoplast. Compos. Mater. 2019, 34, 929–951.
33. Pigliaru, L.; Rinaldi, M.; Ciccacci, L.; Norman, A.; Rohr, T.; Ghidini, T.; Nanni, F. 3D printing of high performance polymer-bonded PEEK-NdFeB magnetic composite materials. Funct. Compos. Mater. 2020, 1, 4.